*Journal of Organometallic Chemistry*, 475 (1994) 247–256



# Generation and gas-phase reactivity of $CoGa^+$

Christian Kronseder [a], Thomas Schindler [a], Christian Berg [a], Roland Fischer [b], Gereon Niedner-Schatteburg [a] and Vladimir E. Bondybey [a]

[a] *Institut für Physikalische und Theoretische Chemie und* [b] *Institut für Anorganische Chemie der Technischen Universität München, Lichtenbergstrasse 4, D-85747 Garching (Germany)*

(Received January 14, 1994)

**Abstract**

Electron impact ionization and subsequent fragmentation of volatile but stable organometallic precursor compounds is used to release naked $CoGa^+$ ions to transfer into and analyse by a high resolution Fourier Transform Ion Cyclotron Resonance (FT-ICR) mass spectrometer. Gas-phase bimolecular reactions of $CoGa^+$ ions with methanol, among others, yield two distinct isomers of $(GaCH_3OH)^+$ with significant internal excitation. *Ab initio* calculations using a density functional approach for $CoGa^+$ and $(GaCH_3OH)^+$ complement the experimental findings.

*Key words:* Cobalt; Gallium; Mass spectrometry; Materials

## 1. Introduction

The gas phase chemistry of metal ions [1] and metal cluster ions [2] has been the subject of growing interest. A large part of this interest stems from the ability of metal atoms and surfaces to catalyse a variety of organic reactions, to "activate" C–H and C–C bonds. Insights into the details of this lowering of activation barriers by metals should enable a better understanding of both homogeneous and heterogeneous catalysis.

The main emphasis thus far has been on investigations of homonuclear transition metal clusters. These can be easily produced by pulsed laser vaporization in the presence of an inert carrier gas [3,4] or by fast atom bombardment (FAB) [5]. In contrast, very little is known about the properties and reactivity of heteronuclear clusters. We have pointed out, and shown experimentally some time ago, that these can also be conveniently generated by laser vaporization of suitable alloys of two separate metal targets [4]. Mixed transition metal dimers have recently been generated by laser vaporization of the desired metal in the vicinity of an ICR cell, and allowing the ions to react with $Fe(CO)_5$ to yield the ligated heteronuclear dimer ions. Ligands were then stripped by collision induced dissociation to obtain the bare cluster cation, whose reactions were then studied [6–12]. Other experimental schemes relying on metal carbonyl precursors have been described [13,14].

In the present study, we investigate an alternative approach: using a volatile, ligated heteronuclear metal cluster, and producing the bare dimer or cluster by stripping the ligands. We have investigated a variety of clusters containing one transition metal and one main group atom. Specifically, we have been successful in generating the $CoGa^+$ and $W_2In^+$ cations in large amounts from ligated clusters specially tailored for this purpose. The details of the cluster ion production and of the reactive investigations of the $CoGa^+$ dimers are described.

The gas phase chemistry of both of the component metal cations, $Co^+$ and $Ga^+$, has been previously investigated. The cobalt monomer cation has been studied by guided ion beam techniques. Endothermic reactions of $Co^+$ with $H_2$ and methane $CH_4$ were found to lead to hydrogen abstraction, yielding mainly $CoH^+$ products. Some $CoCH_2^+$ and $CoCH_3^+$ were also found [15]. Another study examined exothermic ammonia as-

Correspondence to: Dr. G. Niedner-Schattenborg.

0022-328X/94/$7.00
*SSDI* 0022-328X(94)24523-L

sociation to $Co^+$ [16]. An increase in the kinetic energy of the cobalt cation leads to an endothermic N–H bond insertion reaction yielding $H–Co^+–NH_2$. In a high pressure flow tube experiment with electronic ground state $Co^+$, the addition of up to three $CH_4$ and two $C_2H_6$ molecules, respectively, to ground state $Co^+$ was found to occur by three body association processes [17]. Propane was found to be the smallest alkane molecule reacting exothermically with $Co^+$ by activating both the C–C and C–H bonds [18]. Exothermic reactions of $Co^+$ with ethylene have been found not to occur [19].

The association reactions of $Ga^+$, as well as of the other Main Group III metal cations, $Al^+$ and $In^+$, with methanol have been investigated by high pressure flow tube experiments. Rate constants for the consecutive association up to three methanols have been determined. The decrease in the rate constants in the order $Al^+ > Ga^+ > In^+$ was interpreted as evidence for the decrease in bond energies in this order [20]. The $(AlMeOH)^+$ cation has been examined by *ab initio* calculations. These found a bond energy of 37 kcal $mol^{-1}$ (1.6 eV) [20]. In a later ICR study, $Al^+$ was reacted with methyl acetate yielding mostly $(AlMeOH)^+$ by the elimination of ketene [21]. A lower limit for the $(AlMeOH)^+$ bond strength of $\geq 38$ kcal $mol^{-1}$, in fair agreement with the theoretical prediction, was found. No reaction of $Ga^+$ with methanol was observed in another ICR study [22]. This might be due to the single collision conditions of ICR investigations preventing rapid collisional thermalization of otherwise metastable product complexes. The rare earth cations $Sc^+$, $Y^+$, and $Lu^+$, isovalent to the Group III cations, exhibit various reaction pathways with methanol that yield metal oxygen bonds, as shown in a recent ICR investigation [23].

Recently, a photodissociation spectroscopy study [24] of metal–water complexes and associated *ab initio* calculations [25] have been performed. The ground state dissociation energy of $Mg^+–H_2O$ was determined to be 1.06 eV [24]. Another *ab initio* calculation results in a bond energy for electrostatically bound acetone which is even higher than that for the covalently bound $CH_3$ [26].

In the case of the reaction of $Fe^+$ with methanol, effectively a metal insertion into the C–O bond was observed. $FeOH^+$ was the only ionic reaction product [27]. O–H bond activation of water and methanol by $Fe^+–CH_3$ was also reported [28]. The ligated iron cation reacts with the polar methanol molecule expelling methane. An attack of the iron at the oxygen atom of the methanol was suggested followed by H-migration from the oxygen atom to the methyl group to finally expel the methane, was observed to miss.

## 2. Method of cluster generation

Organometallic compounds containing a heteronuclear metal core have recently been synthesized as single source precursors for CVD application [29]. These compounds fullfil certain requirements such as volatility and thermal stability to allow for electron impact ionization studies. We systematically checked some of these compounds to find out whether they fragment in part into bare metal clusters of appropriate stoichiometries. Electron impact energies were kept at 70 eV, whereas the vaporization temperatures were adjusted for each compound to obtain strong ion signals while avoiding thermal decomposition (60–90°C).

Initial attempts concentrated on four compounds containing a central iron gallium dimer. Ligands were chosen to shield the reactivity of the dimer effectively while allowing easy fragmentation by boiling off the ligands after electron impact (EI) ionization. Cyclopentadienyl (cp), carbonyl (CO), ethyl (Et), n-propyldimethylamine ($^nPrNMe_2$), tetrahydrofurane (THF), chloride (Cl) and boronetetrahydride ($BH_4$) were among the ligands that were used. The four compounds studied were $cpFe(CO)_2–Ga(Et)^nPrNMe_2$ (**1**), $cpFe(CO)_2–Ga(Cl)^nPrNMe_2$ (**2**), $cpFe(CO)_2–GaCl_2$-$NMe_3$ (**3**), and $cpFe(CO)_2–Ga(BH)_4{}^nPrNMe_4$ (**4**). The EI fragmentation spectra of the four compounds showed no occurrence of naked $FeGa^+$. Compound **2** resulted in some fragments where gallium was lost, but its propylamine ligand switched positions to the iron cation. Compound **3** had the highest rate of Fe–Ga bond cleavage. Compound **4** yielded some fragments containing only the gallium ligands (and their fragments). These presumably formed by strong $\cdots(B–N)\cdots$ bonding. For all four compounds, the smallest fragment containing an intact Fe–Ga cluster had at least the cp ligand remaining on the iron. From this, one may conclude that the cp–Fe bond is significantly stronger than the Fe–Ga bond.

Two cobalt–gallium complexes were investigated, $(CO)_4Co–GaEt_2(NMe_3)$ (**5**) and $(CO)_4Co–GaCl_2(THF)$ (**6**) [30]. Both yielded rather strong $CoGa^+$ cluster peaks at 128 a.m.u. The observed fragmentation pattern reveals that all of the metal ligand bonds present are about as strong as the cobalt–gallium bond. This thus must be more stable than the Fe–Ga bond in the above complexes. In the case of **5**, two almost equally abundant fragments $GaEt_2^+$ at 127 a.m.u. and $CoGaH^+$ at 129 a.m.u. obscure this mass region somehow. The capabilities of the FT-ICR instrument permit the isolation of the desired $CoGa^+$ cluster by ejection of all of the other fragments, but at the expense of the intensity and unwanted rf-heating. In the case of **6**, the $CoGa^+$ fragments are not obscured by other fragments, allow-

ing easy selection. The reactive investigations described in the following section were performed using this approach.

Since we had the relatively volatile trinuclear $[(CO)_3Wcp]_2$–$In(^nPrNMe_2)$ complex (7) available, we also examined its fragmentation pattern. The strongest peak in the EI ionization spectrum is $In^+$. It was ejected from the cell prior to detection of the fragments. The strongest fragment is the parent ion. Fragments result in part from the cleavage of the W–In bond, in part from the pairwise concerted loss of tungsten ligands. The naked $WInW^+$ cluster still exhibits a considerable intensity (15% of the parent) and might be a linear triatomic molecule as one can conclude from the fragmentation pattern. It would certainly be possible to use it for reactive investigations.

## 3. Experimental details

The screening presented above as well as the reactive investigations presented in the following were performed by a Fourier transform ion cyclotron resonance, FT-ICR, spectrometer (Spectrospin CMS 47X) equipped with a superconducting 4.7 T magnet, a cylindrical $60 \times 60$ mm$^2$ ICR cell and a differentially pumped external electron impact ion source. The $CoGa^+$ cluster was produced by electron impact ionization (30 eV) of **6** vaporized at 65°C in the external ion source. Cluster and fragment ions were extracted and transferred into the ICR cell by means of electrostatic ion optics. The $CoGa^+$ was obtained in 27% yield of the most intensive fragment peak $(CO)CoGaCl_2^+$.

For the reactive investigations, all ions but the desired $CoGa^+$ were eliminated by resonant rf irradiation at their respective resonant cyclotron frequencies. Neutral reactants were introduced into the UHV region *via* a needle valve and maintained at a constant pressure of about $10^{-8}$ mbar to ensure single collision conditions. The methanol and water reactants were purified by several freeze-pump-thaw cycles before use in order to minimize air contaminants. Variation of the reaction delay prior to product detection yielded temporal reaction profiles such as that displayed in Fig. 1. Pseudo first order kinetics were simulated numerically while adjusting the individual reaction rate constants until a satisfactory agreement was found with the experimental findings. These relative rate constants and branching ratios were brought to an absolute scale by careful neutral reactant number density calibration as described elsewhere [31]. Reaction efficiencies were computed by comparison with collision rate constants from suitable theoretical predictions [32].

A number of collision induced dissociation (CID) experiments were carried out to obtain some information about the ion binding and structures. Considerable care was taken to assure that the investigated ions were well thermalized (see Fig. 2). After selecting the ion of interest, a pulse of an inert gas was introduced *via* a piezoelectric valve. This raised the pressure to a maximum value of $10^{-5}$ mbar. During the pressure rise of approximately 1 s duration, the trapped ions underwent about 400 collisions. Since these thermalizing collisions introduced some fragmentation, the remaining ion of interest was then reselected. It was then excited to the desired kinetic energy [33] for the actual CID experiment. This was performed by introducing a second argon gas pulse. Finally, after a suitable delay, the remaining ions and their fragments were mass analyzed.

## 4. Results of $CoGa^+$ reactions

The reactions of the heteronuclear cluster cation $CoGa^+$ are listed in Table 1. No reactions of $CoGa^+$ with $CH_4$, $C_2H_4$, $C_2H_6$, $(C_2H_5)_2O$, $N_2$, $O_2$, $H_2$, CO and NO were detected. Typical reaction times of 10 s yield a lower limit for the rate constants of $10^{-14}$ cm$^3$ s$^{-1}$, or reaction efficiencies of less than 1 in $10^5$ collisions. As noted above, the $Co^+$ monomer does not undergo any exothermic reaction under single collision conditions with those small molecules used here either. No addition of methane or ethylene with elimination of Ga was observed. In a high pressure flow tube experiment, addition of these molecules to $Co^+$ has been observed [17], nevertheless.

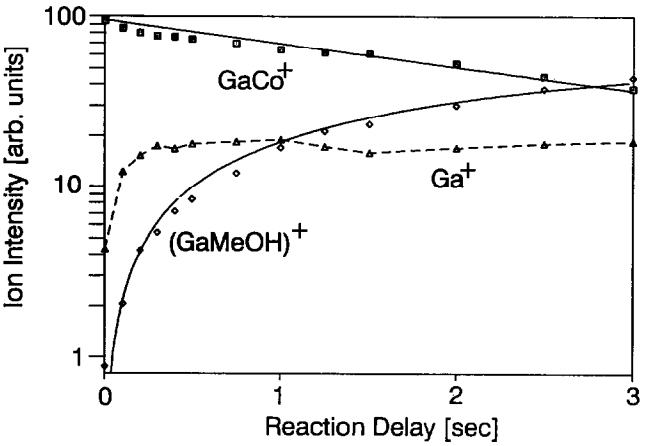


Fig. 1. Temporal reaction profile of the reaction of $CoGa^+$ cluster with methanol at a corrected pressure of $4.9 \times 10^{-8}$ mbar. Initial fragmentation of the kinetically and internally excited cluster ion leads to fragmentation in $Ga^+$ and neutral Co. The $Ga^+$ signal then remains constant indicating that no further production and no reaction of $Ga^+$ with methanol proceeds.

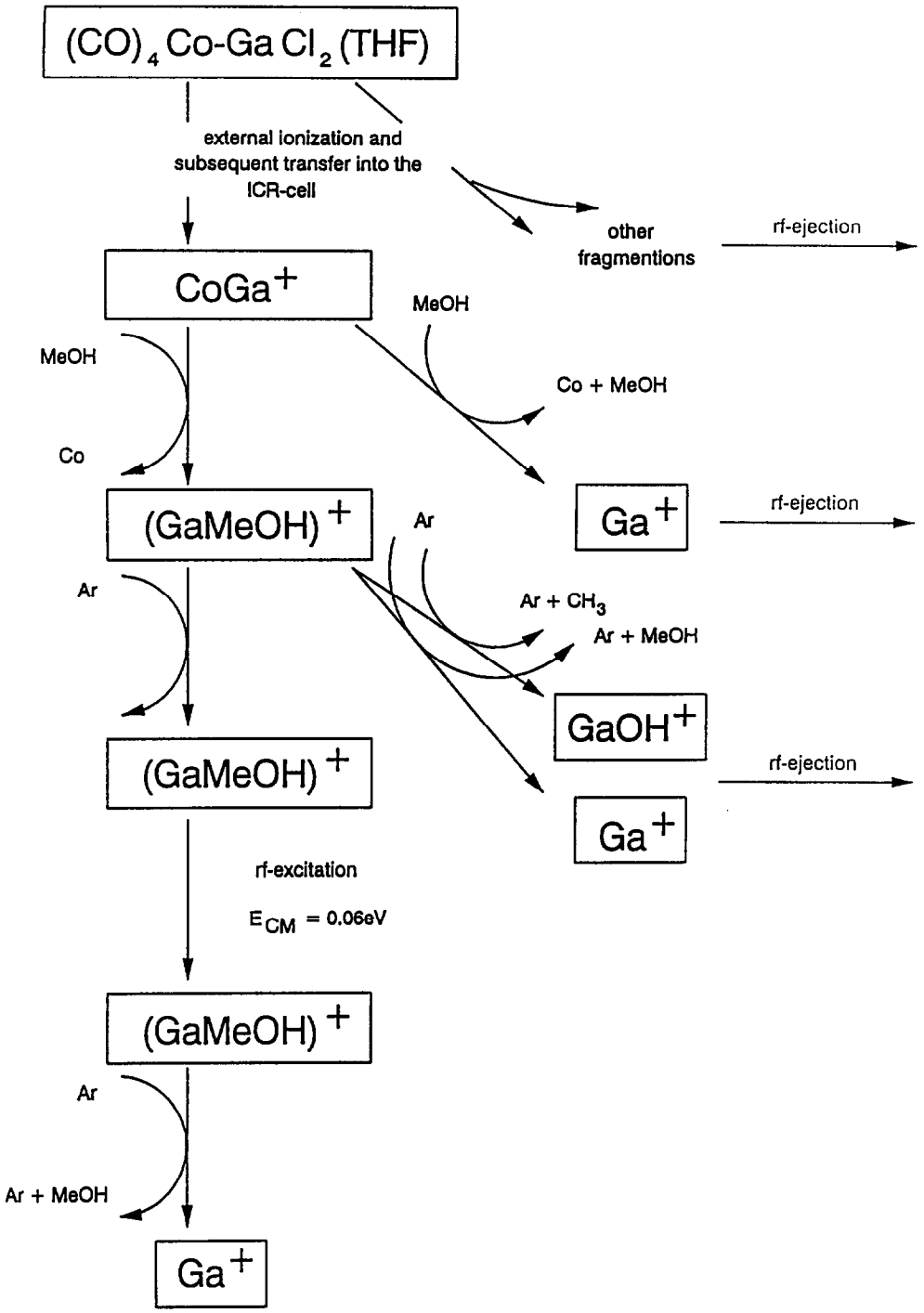


Fig. 2. Graphical representation of the experimental cycle to determine the structure of $(GaMeOH)^+$, the ionic product of the reaction of the $CoGa^+$ cluster with methanol. $CoGa^+$ is produced by electron impact ionization of the organometallic compound $(CO)_4CoGaCl_2(THF)$ in the external ion source of our FT-ICR. The cluster and various fragment ions are then transferred to the ICR cell where the cluster ion is isolated by rf-ejection of the fragments. Reaction with methanol leads to $(GaMeOH)^+$. To obtain structural information of this reaction product, collision induced dissociation (CID) experiments were performed. A first CID experiment on the internally and kinetically hot reaction product shows $GaOH^+$ and $Ga^+$ as fragment ions indicating a metal insertion reaction. A subsequent CID experiment on the yet thermalized ion with controlled rf-excitation results in $Ga^+$ as ionic fragment. This suggests an electrostatic bonding of $Ga^+$ with methanol.

Reactions were observed to proceed with $CH_3OH$, $H_2O$ and $NH_3$. Dissociative attachment was the dominating process of $CoGa^+$ exposure to ammonia leading mainly to $(GaNH_3)^+$ and to a small fraction of $(CoNH_3)^+$. The total rate constant of the reaction was determined to be $(3.7 \pm 1.3) \times 10^{-10}$ cm$^3$ s$^{-1}$. Comparison with the theoretical collision rate (ADO rate) [32] under assumption of thermal energies leads to an overall reaction efficiency of 22%. Reaction of $CoGa^+$ with water forming $(GaH_2O)^+ + Co$ proceeds with a rate constant of $(2.3 \pm 0.9) \times 10^{-10}$ cm$^3$ s$^{-1}$. The reaction efficiency was 13%.

An analogous association reaction of $CoGa^+$ was observed with methanol. Figure 1 illustrates the temporal profile of this reaction. Initial fragmentation of some hyperthermal $CoGa^+$ results in $Ga^+$ fragments. $Ga^+$ itself does not show any further reactions with methanol, which was confirmed separately. The total rate constant of $CoGa^+ + CH_3OH \rightarrow (GaCH_3OH)^+ + Co$ was determined to be $(1.9 \pm 0.5) \times 10^{-10}$ cm$^3$ s$^{-1}$, corresponding to a reaction efficiency of 12%.

To elucidate the structure of the reaction product, collision-induced dissociation experiments (CID) were performed very much as outlined above (see Fig. 2). The $(GaCH_3OH)^+$ product cation was reselected. Subsequent collisions with argon yielded the fragmentation products $GaOH^+$, $Ga^+$ and some $(GaMeOH)^+$ remaining. The latter was allowed to collide further with the inert buffer gas and reselected. A second CID process with controlled excitation energy of at least 60 meV (centre of mass frame) led to fragmentation of $(GaMeOH)^+$ into $Ga^+$ exclusively.

## 5. Computational results on CoGa and $CoGa^+$

Neither experimental nor theoretical information on CoGa and $CoGa^+$ were available when the present investigations were started. Thus, we performed some approximate *ab initio* calculations by means of a standard density functional approach (program DGAUSS) [34]. The double-zeta split-valence plus polarization (DZVP) basis set of Gaussian-type orbitals incorporated a (63321/531/41) basis at the cobalt and a (63321/5321/41) basis at the gallium. These basis sets are, however, optimized for use within the so-called local spin density (LSD) approximation [35]. These LSD-optimized Gaussian basis sets are claimed to cause only small basis set superposition errors (BSSE) [34]. Geometrical parameters as calculated by density functional approaches are quite accurate in general [34]. In contrast, the local density approximation tends to overestimate dissociation energies by up to a factor of two [36]. Non-local exchange-correlation corrections (non-local spin density, NLSD) as applied in the present study help to reduce this problem [37–39]. Impressive agreement between the corrected values and exact experimental and/or theoretical energies has been achieved for molecules involving light atoms only [34]. No information is available on the estimated accuracies when heavy atoms such as transition metals and main group elements are involved.

We started performing some checking calculations on the AlCu heterodimer. Reliable experimental [40] and theoretical values [41] are available for this molecule. The present and previous results are summarized in Table 2. As expected, the computed equilibrium bond distances agree very well whereas the binding energies are somewhat overestimated by the density functional approach. The non-local corrections reduce the discrepancy considerably. Quite reasonable agreement is found on the vibrational fundamental. Thus, we have to retain some caution in the interpreta-

TABLE 2. Comparison of previous and present data on AlCu

| | Total energy (a.u.) | $r_e$ (Å) | $D_e$ (eV) | $\omega_e$ (cm$^{-1}$) |
|---|---|---|---|---|
| Exp. [40] | – | – | 2.25 | 292.2 |
| SCF-CI [41] | −1881.803007 | 2.371 | 2.06 | 289 |
| SCF-CI + R.C. [a] | −1896.365734 | 2.329 | 2.29 | 282 |
| LSD | −1878.798923 | 2.3287 | 3.11 | n.a. |
| NLSD | −1882.882198 | 2.3287 [b] | 2.74 | 315 |

[a] Relativistic corrections. [b] Geometry was optimized at the LSD level only.

TABLE 1. Reactions of the $CoGa^+$ cluster cation with some small molecules (the reaction efficiency is given with respect to the theoretical collision rate (ADO rate) [32])

| Reaction | Reactive rate constant (cm$^3$ s$^{-1}$) | Reaction efficiency |
|---|---|---|
| $CoGa^+ + CH_4, C_2H_4, C_2H_6, (C_2H_5)_2O, N_2, O_2, H_2$, CO, NO | $< 10^{-14}$ | – |
| $CoGa^+ + NH_3 \rightarrow (GaNH_3)^+ + Co \rightarrow (CoNH_3)^+ + Ga$ | $(3.7 \pm 1.3) \times 10^{-10}$ | 0.22 |
| $CoGa^+ + H_2O \rightarrow (GaH_2O)^+ + Co$ | $(2.3 \pm 0.9) \times 10^{-10}$ | 0.13 |
| $CoGa^+ + MeOH \rightarrow (GaMeOH)^+ + Co$ | $(1.9 \pm 0.5) \times 10^{-10}$ | 0.12 |

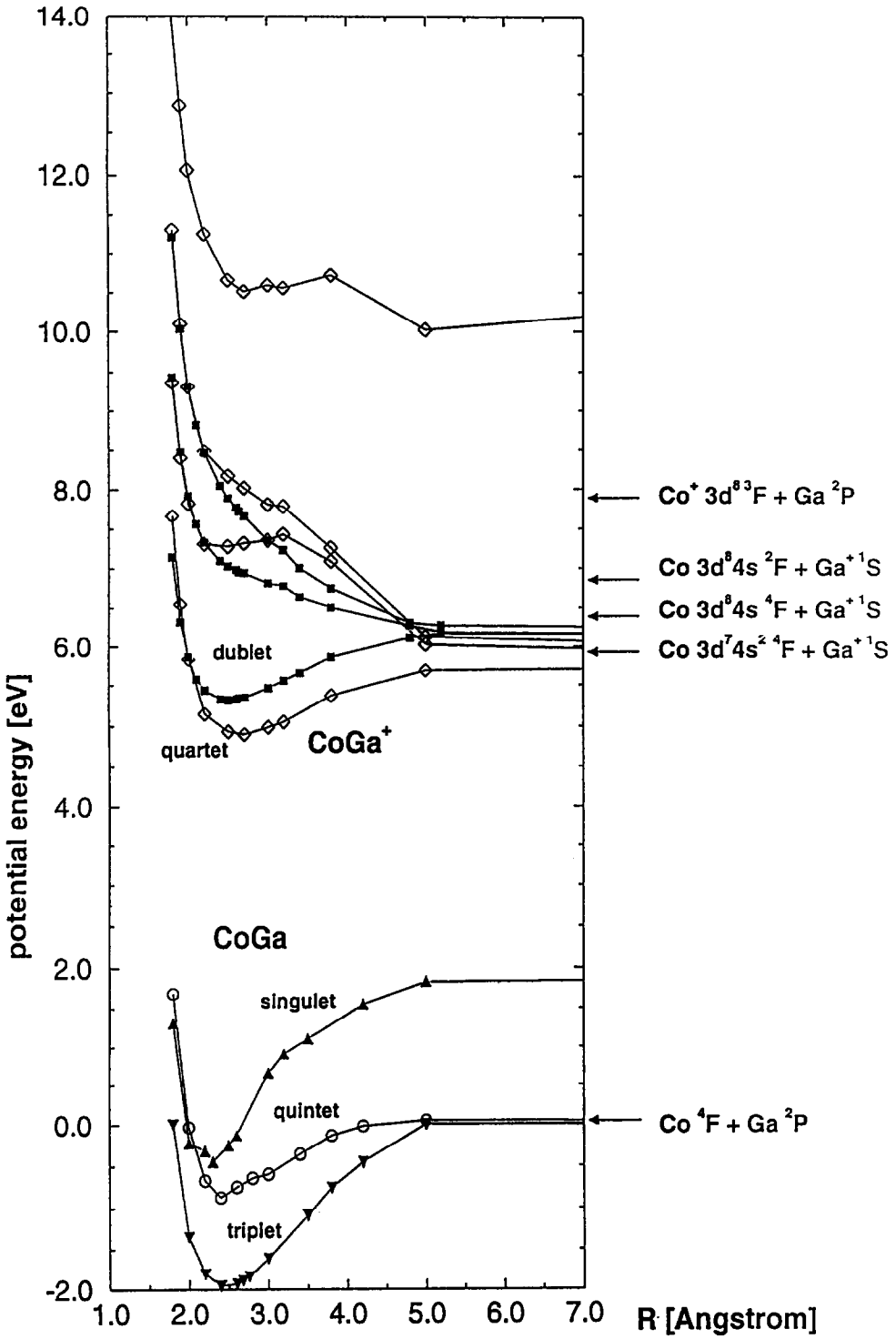


Fig. 3. Computed potential energy curves of CoGa and of $CoGa^+$. The neutral CoGa is most stable in triplet configuration with low lying quintet and singlet excited states. The equilibrium bond lengths are similar for all three states. The cationic $CoGa^+$ is weakly bound in its quartet and doublet states, the latter being slightly more stable. The adiabatic and vertical ionization potentials of CoGa are both computed to be about 7.88 eV compared to 8.11 eV in Co and 6.13 eV in Ga. The experimental ionization potentials are 7.86 eV and 6.00 eV, respectively. Thus, the positive charge in the dimer is expected to localize preferentially on the gallium atom.

tion of energetic values from the LSD/NLSD calculations whereas the geometrical parameters are believed to be reliable.

With the present knowledge, we performed far more extensive calculations on the CoGa heterodimer and its cation. We not only searched for the equilibrium bond distance but calculated multiple off-equilibrium distances in order to learn about the entire potential wells and its volumes and shapes. The results are summarized in Fig. 3 and Table 3. The neutral heterodimer CoGa is most stable in triplet configuration with low lying quintet and singlet excited states. The equilibrium bond lengths are similiar for all three states. The binding energy of the quintet state is about half those of the singlet and triplet states which are of comparable strength. In the homogeneous dimer $Ga_2$, the equilibrium bond distance is slightly larger (2.72 Å [42]) than in CoGa and the bond is weaker ($D_0 = 1.4$ eV, [42]). No measurements or predictions have been published for $Co_2$.

The cationic $CoGa^+$ molecule is weakly bound both in its quartet and doublet states, the latter being slightly more stable. The adiabatic and vertical ionization potentials of CoGa are both computed to about 7.88 eV to compare to 8.11 eV in Co and 6.13 eV in Ga. The experimental ionization potentials are 7.86 eV and 6.00 eV, respectively [43]. Thus the positive charge in the dimer is expected to localize preferentially on the gallium atom. Also the computed potential curves dissociate towards multiple $Co + Ga^+$ states (cf. Fig. 3) while the lowest $Co^+ + Ga$ state is way off.

The above data have yielded reasonable structures and energies for both the AlCu and the CoGa dimers which contain two heavy metal atoms each. A previous article had demonstrated the accuracy of such computations for small organic molecules [34]. There the DZVP basis set was extended by p-polarization functions at the H-atoms (DZVPP). The corresponding Pople basis sets would be 6-31G* and 6-31G**, respectively. We compared both sets, DZVP and DZVPP, in the case of methanol and found minor geometrical deviations which were negligible when compared to the (in general small) variance with respect to experimental values. Thus, we felt encouraged to extend the density functional approach to the present major product complexes while using the DZVP basis sets.

TABLE 3. Computed data on CoGa and $CoGa^+$

| | Total energy (a.u.) | $r_e$ (Å) | $D_e$ (eV) |
|---|---|---|---|
| CoGa | | | |
| Triplet | −3307.477905 | 2.50(5) | 2.33 |
| Quintet | −3307.437957 | 2.4(1) | 0.87 |
| Singlet | −3307.382937 | 2.3(1) | 2.25 |
| $CoGa^+$ | | | |
| Quartet | −3307.224300 | 2.70(5) | 0.78 |
| Doublet | −3307.210161 | 2.48(5) | 0.50 |

TABLE 4. Computed parameters of $(GaCH_3OH)^+$ complexes (geometrical parameters are optimized at LSD level of theory; energies include non-local spin density corrections (NLSD))

| | $Ga^+ + CH_3OH$ | $Ga^+CH_3OH$ | $CH_3Ga^+OH$ |
|---|---|---|---|
| Total energy (a.u.) | −2040.21923 | −2040.26671 | −2040.24183 |
| Relative energy (eV) | 0 | −1.29 | −0.68 |
| Distances (Å) | | | |
| Ga–O | – | 2.150 | 1.710 |
| Ga–C | – | – | 1.877 |
| C–O | 1.410 | 1.454 | – |
| O–H | 0.977 | 0.985 | 0.987 |
| C–H | 1.110 | 1.103 | 1.106 |
| Angles (°) | | | |
| C–O–H | 108.2 | 110.1 | – |
| H–C–H [a] | 107.9 | 110.0 | 110.7 |
| Ga–O–C | – | 128.2 | – |
| O–Ga–C | – | 169.4 | – |
| Mulliken charges | | | |
| Ga | 1 | 0.737 | 0.710 |
| O | −0.526 | −0.568 | −0.616 |
| C | −0.551 | −0.523 | −0.557 |
| H (at O) | 0.417 | 0.504 | 0.506 |
| H (at C) [a] | 0.220 | 0.283 | 0.319 |

[a] Average values.

We investigated methanol and gallium cation at very large distance, $Ga^+ + CH_3OH$ (**8**), gallium cation attached to methanol at the oxygen atom, $Ga^+CH_3OH$ (**9**), and gallium inserted into the C–O bond of methanol, $CH_3Ga^+OH$ (**10**). Geometries were optimized in each case at the LSD level of theory as was applied to the CoGa dimer. Final corrections for non-local spin density (NLSD) effects have been included in the total energies. The results are summarized in Table 4. While the energies are thought to establish upper limits for the true binding energies, the computed geometries are believed to be of significant accuracy.

The computed binding energies with respect to desorption of an intact methanol molecule favour the non-inserted structure **9** over the inserted structure **10** by a factor of two. The dissociation energy of methanol into $CH_3$ and OH is known by the heat of formation to be 4.10(±0.04) eV [43]. Thus, the consecutive adsorption of a $CH_3$ unit and of an OH unit on a gallium cation yields an energy gain equalling this value plus the computed binding energy of structure **10**, 0.68 eV.

Together both units are thus bound to the gallium by (at most) 4.78 eV. The stabilization energy is of course shared by the two bonds.

The non-inserted complex **9** is of oxonium type structure. The presence of the gallium cation induces considerable electronic reorganization with respect to an isolated methanol molecule. This manifests itself in the analysis of Mulliken charge distributions (cf. Table 4). The gallium cation transfers about a third of its nominal charge to the methanol where it is distributed about equally to the four hydrogen atoms. The electronegative carbon and oxygen atoms maintain their negative partial charges. Thus, complexation of methanol with gallium cations into the oxonium structure **9** performs by a flux of electron density from the peripheral hydrogen atoms through the central electrophils into the O–Ga bond. Computed numeric values of the partial charges are included in Table 4. Although the general trends are doubtlessly correct, the numeric values probably reveal bonds which are slightly more strongly polarized than actually observed (as e.g. in AlCu).

## 6. General discussion

In our experiments, no reactions with $CH_4$, $C_2H_6$, $C_2H_4$, $(C_2H_5)_2O$, $N_2$, $O_2$, $H_2$, CO and NO have been observed although it is known that cobalt cations react, e.g. with $CH_4$ in drift tubes [44], and with $C_2H_5$ [1] or $(C_2H_5)_2O$ [45]. On the other hand, little is known about the reactions of bare main group metal cations in the gas phase.

The seemingly severe discrepancy between previous high pressure investigations of cobalt cations to react easily with non-polar hydrocarbon molecules and the present single collision studies of $CoGa^+$ hetero dimers to refrain from such reactions is not attributed to any kind of gallium driven inhibition. It is believed, however, to reflect the difference in principle, between multiple and three body collision induced metastable complex stabilization at high pressures on the one hand and preferential direct association and replacement processes without third bodies present on the other hand.

In contrast, metastable electrostatically bound complexes of $CoGa^+$ with polar molecules may not form only temporarily. These complexes stabilize without further collisions if the stabilization energy exceeds the $CoGa^+$ dissociation energy. Then either of the metal atoms may expel in principle. Due to their higher ionization potential, neutral cobalt atoms are preferred to leave the complex. Observation of some $CoNH_3^+$ complexes in addition to $GaNH_3^+$ shows that the metal cation-ammonia binding energy is about equal to the

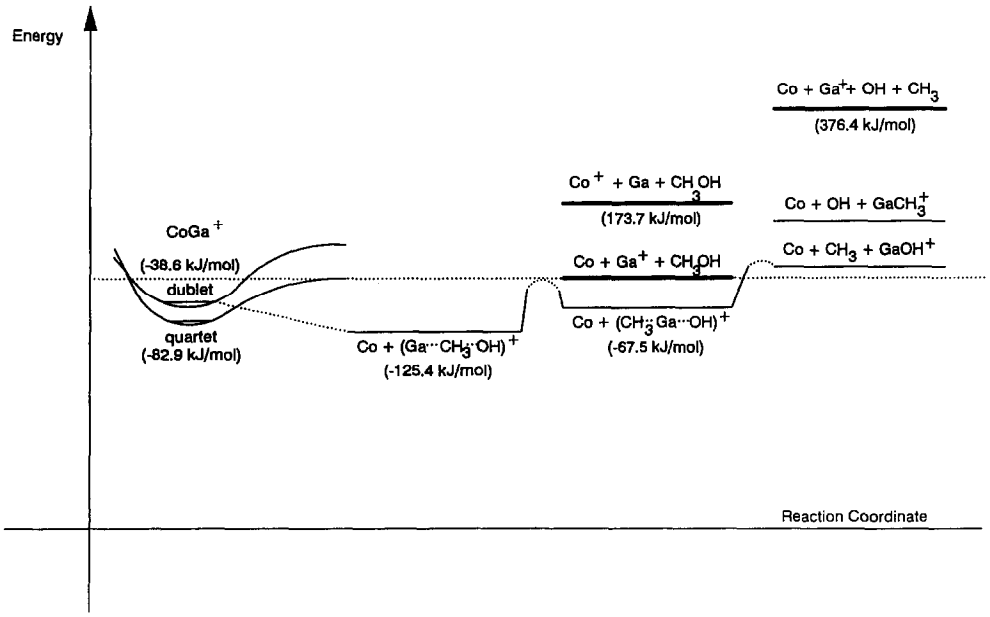


Fig. 4. Relative energetics of each reaction channel with respect to $\Delta H_f(Co + Ga^+ + CH_3OH)$. Bold solid lines indicate previously well established energies, whereas plain lines indicate those which had to be evaluated in the present investigation. The $GaCH_3^+$ channel seems to be higher in energy than the $GaOH^+$ since the latter is observed, whereas the former is not, although no exact values about the difference in energy can be obtained.

difference in ionization potential of Co and Ga (1.86 eV).

Water and methanol do not stabilize with $Co^+$ while expelling gallium atoms because they are less strongly bound to the metal atoms. For a more comparative view on the very nature of the observed complexes, both the differences in the $Co^+$-molecule and $Ga^+$-molecule complexation, namely acceptor-donor interactions, have to be elucidated. This is discussed in the case of methanol in the following.

Most interesting in the current context are the $CoGa^+$ reactions, especially with $CH_3OH$. The initial fragmentation of the cluster due to multiple collisions with methanol indicates that the cluster carries significant internal energy. In Fig. 4 the relative energetics of each reaction channel with respect to $\Delta H_f(Co + Ga^+ + CH_3OH)$ are shown. Bold solid lines indicate previously well established energies, whereas plain lines indicate those which had to be evaluated by the present investigation. The $GaCH_3^+$ channel seems to be higher in energy than the $GaOH^+$ since the latter is observed whereas the former is not, although no exact values about the difference in energy can be obtained. We determined experimentally the dissociation energy of $Ga^+$–OH, $D_0 < 3.97$ eV in, albeit trivial, agreement with the theoretical value of 1.17 eV. The observation of $(GaMeOH)^+$ indicates that $D_0(CoGa^+) < D_0(Ga–MeOH^+)$.

The two stage CID experiment (cf. Fig. 2) of $CoGa^+ + CH_3OH$ revealed an approximate value of the dissociation energy of the current $(GaCH_3OH)^+$ intermediate of about 60 meV (+60 meV/−20 meV). Little energy is necessary to split the complex, although both $CoGa^+$ and $(GaMeOH)^+$ are thought to be bound stronger than just 60 meV. We conclude that internal (vibrational) excitation of the product complex $(GaCH_3OH)^+$ accounts for the difference between theoretically predicted and experimentally observed energy.

Theory reveals an excited doublet state of $CoGa^+$, which may be populated in the course of electron impact ionization and fragmentation of the precursor molecule. The dissociation threshold of the doublet state is about 400 meV higher in energy than that of the quartet ground state. This value is even twice as high (923 meV) if the computed curves are scaled to the exact dissociation limits. The doublet potential well is entirely above the quartet threshold. Thus, doublet $CoGa^+$ may well be metastable. The computed stabilization of $CoGa^+$ in its doublet state with respect to the isolated atoms $Co + Ga^+$ in their ground states of 436 meV is an upper bound. The true value may be significantly lower or even negative.

Collision with either unreactive (Ar) or reactive ($CH_3OH$) partners are operative in coupling the two $CoGa^+$ states and thus inducing intersystem crossing from the doublet state into vibrationally highly excited quartet levels and into direct dissociation on the quartet potential.

In summary, Ar collisions thus lead to dissociation and population of hot quartet states exclusively, while methanol may scavenge gallium cations in part and may also predissociate otherwise bound $CoGa^+$ quartet vibrational levels by virtue of the considerable stabilization energy gain in the $(GaMeOH)^+$ complex. The resulting $(GaMeOH)^+$ is vibrationally hot in itself, of course, since the neutral Co does not carry away all of the excess energy.

$(GaMeOH)^+$ is an ion-dipole bound complex that forms from $CoGa^+$ without a significant activation barrier. The opposite is true for the inserted structure which more weakly bound and where considerable activation takes place. Both structures are distinguishable by fragmentation patterns generated by CID experiments. $GaOH^+$ is believed to form only from **10**. The double CID experiments as performed yield this fragment only in the former CID experiments whereas the latter yields only $Ga^+$ fragments. We interpret this finding as an initially parallel occurrence of both structures. Thus, all of the experimental findings are very much in line with the theoretical predictions and *vice versa*.

## 7. Conclusions

We have shown that certain organometallic compounds may well release dinuclear metal cations upon electron impact ionization. This also holds for systems with metal bonds that are far from tight bonding. From this fact one can draw implications for hot wall CVD processes that run with such compounds. Bimetallic layers can thus form, for example from pure gas phase hetero dimers without significantly incorporating sticky ligands.

The gas phase reactions such as performed yield strong evidence for internal excitation of the electron impact ionization and fragmentation generated $CoGa^+$ cations. The *ab initio* results suggest metastable electronic states of doublet multiplicity to bear this excitation. Computed and optimized equilibrium geometries and heat of formations of the $(GaMeOH)^+$ isomers provide final support for the picture presented.

**Acknowledgement**

This work was supported by the Deutsche Forschungsgemeinschaft and by the Fond der chemischen Industrie.

## References


1 K. Eller and H. Schwarz, *Chem. Rev.*, *91* (1991) 1121.
2 D.C. Parent and S.L. Anderson, *Chem. Rev.*, *92* (1992) 1541.
3 T.G. Dietz, M.A. Duncan, D.E. Powers and R.E. Smalley, *J. Chem. Phys.*, *74* (1981) 6511.
4 V.E. Bondybey and J.E. English, *J. Chem. Phys.*, *74* (1991) 6978.
5 M.P. Irion and P. Schnabel, *Ber. Bunsenges. Phys. Chem.*, *96* (1992) 1091.
6 L.M. Lech, J.R. Gord and B.S. Freiser, *J. Am. Chem. Soc.*, *111* (1989) 8588.
7 R.L. Hettich and B.S. Freiser, *J. Am. Chem. Soc.*, *107* (1985) 6222.
8 (a) D.B. Jacobson and B.S. Freiser, *J. Am. Chem. Soc.*, *108* (1986) 27; (b) D.B. Jacobson and B.S. Freiser, *J. Am. Chem. Soc.*, *106* (1984) 4623.
9 E.C. Tews and B.S. Freiser, *J. Am. Chem. Soc.*, *109* (1987) 4433.
10 Y. Huang, S.W. Buckner and B.S. Freiser, in P. Jena, B.K. Rao and S.N. Khanna (eds.), *Physics and Chemistry of Small Clusters*, Plenum Press, New York, 1987.
11 Y. Huang and B.S. Freiser, *J. Am. Chem. Soc.*, *110* (1988) 387.
12 S.W. Buckner and B.S. Freiser, *J. Phys. Chem.*, *93* (1989) 3667.
13 Y.H. Pan and D.P. Ridge, *J. Phys. Chem.*, *93* (1989) 3375.
14 Y.H. Pan and D.P. Ridge, *J. Am. Chem. Soc.*, *113* (1991) 2406.
15 P.B. Armentrout and J.L. Beauchamp, *J. Am. Chem. Soc.*, *103* (1981) 784.
16 D.E. Clemmer and P.B. Armentrout, *J. Am. Chem. Soc.*, *111* (1989) 8280.
17 R. Tonkyn, M. Ronan and J.C. Weisshaar, *J. Phys. Chem.*, *92* (1988) 92.
18 P.A.M. van Koppen, J. Brodbelt-Lustig, M.T. Bowers, D.V. Dearden, J.L. Beauchamp, E.R. Fisher and P.B. Armentrout, *J. Am. Chem. Soc.*, *113* (1991) 2359.
19 P.B. Armentrout and J.L. Beauchamp, *J. Chem. Phys.*, *74* (1981) 2819.
20 R.E. Leuchtner, R.W. Farley, A.C. Harms, H. Funasaka and A.W. Castleman, Jr., *Int. J. Mass. Spectrom. Ion Proc.*, *102* (1990) 199.
21 J.S. Uppal and R.H. Staley, *J. Am. Chem. Soc.*, *104* (1982) 1229, 1235.
22 A.K. Chowdhury and C.L. Wilkins, *Int. J. Mass Spectrom. Ion Proc.*, *82* (1988) 163.
23 M. Azzaro, S. Breton, M. Decouzon and S. Geribaldi, *Int. J. Mass Spectrom. Ion Proc.*, *128* (1993) 1.
24 K.F. Wiley, C.S. Yeh, D.L. Robbins, J.S. Pilgrim and M.A. Duncan, *J. Chem. Phys.*, *97* (1992) 8886.
25 C.W. Bauschlicher, Jr., M. Sodupe and H. Partridge, *J. Chem. Phys.*, *96* (1992) 4453.
26 C.W. Bauschlicher and H. Partridge, *Chem. Phys. Lett.*, *181* (1991) 129.
27 J. Allison and D.P. Ridge, *J. Am. Chem. Soc.*, *98* (1976) 7445.
28 O. Blum, D. Stöckigt, D. Schröder and H. Schwarz, *Angew. Chem. Int. Ed. Engl.*, *31* (1992) 603.
29 (a) R.A. Fischer, J. Behm, E. Herdtweck and C. Kronseder, *J. Organomet. Chem.*, *437* (1992) C29; (b) R.A. Fischer, J. Behm, T. Priermeier and W. Scherer, *Angew. Chem.*, *105* (1993) 776; (c) R.A. Fischer, T. Priermeier and W. Scherer, *J. Organomet. Chem.*, *459* (1993) 65; (d) R.A. Fischer, J. Behm, T. Priermeier, E. Herdtweck and W. Scherer, *Inorg. Chem.*, *33* (1994) in press.
30 D.J. Patmore and W.A.G. Graham, *Inorg. Chem.*, *5* (1996) 1586.
31 T. Schindler, C. Berg, G. Niedner-Schatteburg and V.E. Bondybey, in preparation.
32 T. Su and M.T. Bowers, in M.T. Bowers (ed.), *Gas Phase Ion Chemistry*, Vol. 1, Academic Press, New York, 1979.
33 (a) M.B. Comisarow, *J. Chem. Phys.*, *55* (1971) 205; (b) A.G. Marshall, *J. Chem. Phys.*, *55* (1971) 1343; (c) M.B. Comisarow and A.G. Marshall, *J. Chem. Phys.*, *64* (1976) 110; (d) A.G. Marshall and D.C. Roe, *J. Chem. Phys.*, *73* (1980) 1581; (e) P. Kofel, M. Allemann, H.P. Kellerhals and K.-P. Wanczek; *Int. J. Mass Spectrom. Ion Proc.*, *74* (1986) 1.
34 J. Andzelm and E. Wimmer, *J. Chem. Phys.*, *96* (1992) 1280.
35 J. Andzelm, E. Radzio and D.R. Salahub, *J. Comput. Chem.*, *6* (1985) 520.
36 T. Ziegler, *Chem. Rev.*, *91* (1991) 651.
37 A.D. Becke, *Phys. Rev. A*, *38* (1988) 3098.
38 A.D. Becke, *ACS Symp. Ser.*, *394* (1989) 165.
39 J.P. Perdew, *Phys. Rev. B*, *33* (1986) 8822.
40 M.F. Cai, S.J. Tsay, T.P. Dzugan, K. Pak and V.E. Bondybey, *J. Phys. Chem.*, *94* (1990) 1313.
41 C.W. Bauschlicher, Jr., R.S. Langhoff and S.P.J. Walch, *J. Chem. Phys.*, *86* (1987) 5603.
42 J. Shim, K. Mandrix and K.A. Gingerich, *J. Phys. Chem.*, *95* (1991) 5435.
43 S.G. Lias J.E. Bartmess, J.F. Liebman, J.L. Holmes, R.D. Levin and W.G. Mallerd, *J. Chem. Phys. Ref. Data*, *17* (1988) Suppl. No. 1.
44 Kemper and M.T. Bowers, *J. Am. Soc. Mass Spectrom.*, *1* (1990) 197.
45 M.A. Tolbert and J.L. Beauchamp, *J. Phys. Chem.*, *90* (1986) 5015.